A cAMP Sensor Based on Ligand-Dependent Protein Stabilization

Mariapaola Sidoli, Ling-chun Chen, Alexander J. Lu, Thomas J. Wandless, and William S. Talbot*

Read Online

ACCESS | Metrics & More | Article Recommendations | Supporting Information

ABSTRACT: cAMP is a ubiquitous second messenger with many functions in diverse organisms. Current cAMP sensors, including Föster resonance energy transfer (FRET)-based and single-wavelength-based sensors, allow for real time visualization of this small molecule in cultured cells and in some cases in vivo. Nonetheless the observation of cAMP in living animals is still difficult, typically requiring specialized microscopes and ex vivo tissue processing. Here we used ligand-dependent protein stabilization to create a new cAMP sensor. This sensor allows specific and sensitive detection of cAMP in living zebrafish embryos, which may enable new understanding of the functions of cAMP in living vertebrates.
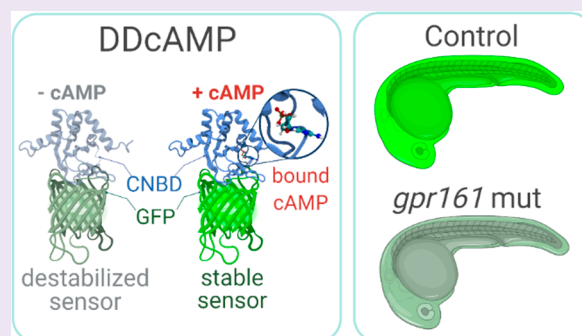
Cyclic adenosine 3′−5′-monophosphate (cAMP) is an essential second messenger that amplifies environmental signals received by G-protein-coupled receptors (GPCRs).[1] The importance of cAMP is underscored by the multitude of physiological processes that it regulates including heartbeat, learning, and memory,[2−4] and it can initiate a wide range of cellular responses including proliferation, differentiation, and death.[5] The kinetics and function of cAMP depend on many factors including the cell type and subcellular compartment where it accumulates and interacts with other signaling molecules,[6,7] which highlights the importance of sensors to visualize cAMP in cultured cells and intact organisms.

Fluorescent sensors for cAMP based on Föster resonance energy transfer (FRET) respond rapidly to local changes in cAMP concentration.[4,8] Although useful in cultured cells, FRET-based sensors are characterized by low signal-to-noise ratio, are prone to photobleaching, and are hampered by light scattering in intact tissues, limiting their use for in vivo imaging.[1,8−10] Single wavelength cAMP sensors using circularly permuted fluorescent proteins, such as Pink Flamindo, R-FlincA, and cAMPr, can mitigate some of the disadvantages of FRET-based sensors.[11−14] Single wavelength sensors have been used to track fast cAMP dynamics in dissected *Drosophila* brains, in *C. elegans* neurons, and in mouse astrocytes.[12,15,16] However, there is often need for dissection and an ex vivo imaging, and it is not clear whether the current tools are useful for long-term imaging.

Ligand-dependent protein stabilization is a strategy that can be used to generate single-wavelength biosensors for small molecules.[17] This approach is based on a protein that is stable only when bound to its cognate ligand.[17−20] This sensor is metabolically unstable and degraded by the proteasome in its unbound state, but engagement by its cognate ligand prevents degradation and leads to a dose-dependent fluorescent signal

when the sensor is fused to an appropriate partner such as GFP. Here we report the application of this approach to develop a genetically encoded single-wavelength cAMP sensor for in vivo imaging using the zebrafish model system (Figure 1; Figure S1).

We sought to identify conditionally stable mutants of the cyclic nucleotide binding domain (CNBD) from the MlotiK1 bacterial channel, which binds cAMP with high specificity and sensitivity in mammalian cells[21,22] (Figure 1A). We started with a codon-optimized CNBD sequence and generated a library of sequence variants using error-prone PCR. This library of CNBD domains was then fused to GFP to enable a cell-based screen for mutants stabilized by cAMP (Figure S1A,B). NIH3T3 cells were stably transduced with the library and subjected to serial rounds of FACS sorting after application or withdrawal of the adenylyl cyclase agonist forskolin (FSK). We selected clones with high GFP signal in the presence of FSK and very low GFP signal in the absence of FSK (Figure S1B). DNA sequencing of selected clones identified many variants encoding unique missense mutations in CNBD, and two variants in particular displayed 3-fold (N41) to 4-fold (N49) increases in GFP intensity upon forskolin treatment (Figure 1B; Figure S1C,D). The N49 variant contains a single mutation in the CNBD domain (Figure S1C,D; blue), whereas N41 contains four mutations
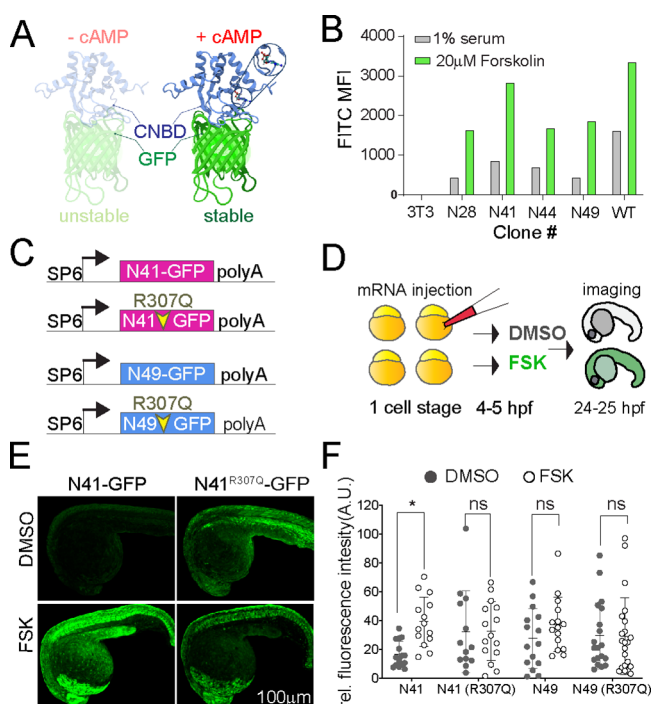
Figure 1. (A) Ribbon diagram of the cAMP sensor composed of CNBD-GFP protein that is unstable without cAMP but stabilized upon cAMP binding: solution structure of a bacterial cyclic nucleotide-activated K$^+$ channel binding domain in cAMP-free form on the left (PBD 2KXL) and bound to cAMP on the right (PBD 2K0G). (B) NIH 3T3 cells stably expressing CNBD-GFP derived from error-prone PCR were treated with 1% serum or 20 μM forskolin for 17 h. (C) Synthetic mRNA encoding the sensor variants N41 and N49 CNBD and the corresponding cAMP-insensitive controls (R307Q). (D) mRNA was injected into zebrafish embryos at the one-cell stage. Embryos were treated at 4−5 hpf with FSK or DMSO for 20 h, then imaged at 24−25 hpf. (E) Representative images showing 24 hpf embryos injected with N41-GFP and N41^{R307Q}-GFP mRNA at one-cell stage and treated with DMSO or 20 μM FSK starting at 4 hpf. (F) Each dot represents mean GFP intensity of one embryo. Error bars indicate SD: *$p < 0.5$ by one-way ANOVA (with Sidák's multiple comparisons), $n = 13−22$ embryos each condition; ns = not significant. AU = arbitrary unit.

spread across the CNBD protein structure (Figure S1C,D; pink).

To test the forskolin responsivity of these CNBD variants in vivo, we injected synthetic mRNA encoding the N41-GFP and N49-GFP sensors into zebrafish embryos, allowing ubiquitous and transient expression of the sensor proteins (Figure 1C,D). Four or five hours after injection of mRNA, we treated embryos with 20 μM FSK for 20 h and subsequently imaged the GFP signal (Figure 1E). Both variants displayed a visible fluorescent signal when expressed in zebrafish embryos, but only N41 increased in response to FSK treatment (Figure 1F). To test whether cAMP binding is required for the response of the N41 variant to forskolin, we compared FSK treatment of N41-GFP with another variant, N41^{R307Q}-GFP, which contains a mutation in a conserved arginine that reduces the efficiency of cAMP binding (Figure 1C; Figure S1C, red circle).[21−23] FSK treatment significantly increased GFP signal in embryos injected with N41-GFP, whereas embryos expressing the cAMP-insensitive N41^{R307Q}-GFP control did not display significant changes in GFP fluorescence (Figure 1E,F). The R307Q mutation appears to stabilize the N41^{R307Q}-GFP

protein, because DMSO-treated N41^{R307Q}-GFP embryos displayed greater GFP signal than DMSO-treated embryos expressing N41-GFP (Figure 1E,F). These analyses provided evidence that the N41-GFP sensor protein is selectively stabilized upon binding to cAMP in vivo, and we hereafter refer to this engineered sensor as DDcAMP (destabilized detector of cAMP).

To further characterize this cAMP sensor, we generated stable transgenic fish lines expressing DDcAMP under control of the regulatory sequences from the ubiquitin gene (abbreviated as *Tg*(*ubi*:DDcAMP), Figure 2A−C), which drives widespread expression in the embryo.[24] As controls, we generated transgenic fish lines expressing ubiquitin-GFP with no CNBD (Figure 2D−F) or the cAMP-insensitive variant DDcAMP^{R307Q} (Figure 2G−I). In situ hybridization demonstrated that the transgenes expressed GFP mRNA at similar levels at 24 h postfertilization (hpf) (Figure 2A,D,G), whereas confocal imaging revealed differences in GFP signal. In contrast to the control transgenes (Figure 2E,F,H,I), embryos expressing the sensor displayed discrete GFP signal localized to the horizontal myoseptum of the somites (Figure 2B,C; white arrows). Quantification confirmed that a region containing muscle pioneers displayed much more GFP signal than a reference area not containing muscle pioneers in *Tg*(*ubi*:DDcAMP) transgenic embryos, but not in embryos expressing the cAMP-insensitive variant cAMP-DDcAMP^{R307Q} (Figure S2C). In *Tg*(*ubi*:DDcAMP) embryos from different transgenic founders and in transgenic embryos expressing the N49 sensor variant *Tg*(*ubi*:N49-GFP), GFP expression was enriched in the muscle pioneers and in the slow superficial fibers (Figure S2Ba−c; yellow arrowheads), cells known to require cAMP signaling for proper specification and differentiation.[25−27] Thus, the comparison of sensor and control transgenic animals provides evidence that DDcAMP is specifically stabilized in a subpopulation of muscle cells.

To test the specificity and sensitivity of DDcAMP to cAMP, we treated *Tg*(*ubi*:DDcAMP) transgenic embryos with FSK for 20 h starting at 4−5 hpf and imaged fluorescent signal in anterior somites using confocal microscopy (Figure 3A,B). FSK significantly increased GFP expression in *Tg*(*ubi*:DDcAMP) but not in *Tg*(*ubi*:DDcAMP^{R307Q}) embryos, and the overall GFP signal in *Tg*(*ubi*:DDcAMP^{R307Q}) embryos was low (Figure 3B). Transgenic sensor animals *Tg*(*ubi*:DDcAMP) showed increased GFP intensity in the enveloping layer (EVL) of the tail (Figure 3C) when treated with increasing concentrations of the cell-permeant cAMP analog 8-cpt-cAMP for 24 h (Figure 3D). The sensor was not activated by treatment with the cGMP analog 8-cpt-cGMP, and treatment with 8-cpt-cAMP did not increase signal in *Tg*(*ubi*:DDcAMP^{R307Q}) control animals (Figure 3D, Figure S3B). Taken together, these experiments provide evidence that DDcAMP is a specific and sensitive sensor for cAMP in the developing embryo.

Time course and time lapse analyses of *Tg*(*ubi*:DDcAMP) indicate that GFP signal appeared in adaxial cells of developing somites at 15 hpf (Movie 1; Figure 3E, red arrow; Figure S3C, white arrows). The signal increased in the somites over time (Figure S3C), pointing to a potential time window of cAMP production during somitogenesis. Further kinetic analyses on *Tg*(*ubi*:DDcAMP) animals showed that the sensor provides a 3-fold increase in fluorescence intensity when treated with FSK for 4 h starting from 14 to 18 hpf (Figure 3F). To compare DDcAMP with the existing cAMP sensor cAMPr,[12] we
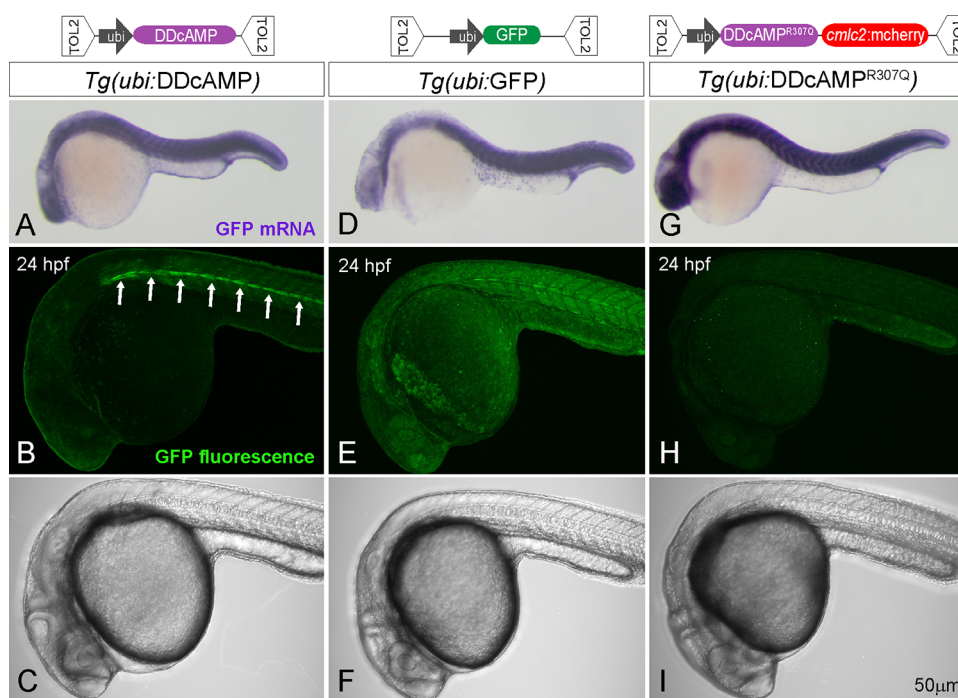
Figure 2. (top) Diagram of the TOL2 plasmids containing N41-GFP, N41^{R307Q}-GFP, and GFP DNA under control of *ubi* promoter. (bottom) In situ hybridization for GFP mRNA in *Tg(ubi:DDcAMP)* (A), *Tg(ubi:GFP)* (D) and *Tg(ubi:DDcAMP^{R307Q})* (G) embryos at 24 hpf. Confocal acquisition of GFP signal in *Tg(ubi:DDcAMP)* (B, C), *Tg(ubi:GFP)* (E, F), and *Tg(ubi:DDcAMP^{R307Q})* (H, I) embryos at 24 hpf. Horizontal myoseptum is indicated by white arrows in panel B.

generated a stable transgenic fish line expressing cAMPr driven by the *ubi* promoter *Tg(ubi:cAMPr)*. Transgenic cAMPr originating from one founder expressed GFP in slow muscle cells, similar to DDcAMP (Figure 3G), whereas cAMPr transgenic fish from another line expressed detectable GFP in skin but not muscle cells (Figure S3D). Signal from cAMPr increases after few minutes of FSK treatment in cell culture,[12] so we examined cAMPr transgenic fish from both founders treated with FSK for times ranging from 15 min to 4 h (Figure 3H, Figure S3D). In contrast to *Tg(ubi:DDcAMP)*, GFP intensity did not significantly increase in response to FSK in *Tg(ubi:cAMPr)* animals at any of these time points (Figure 3H).

Previous studies show that cAMP regulates muscle cell specification.[25,26] In zebrafish, secretion of Sonic Hedgehog (Shh) from the notochord instructs adjacent adaxial cells to differentiate into muscle pioneers, slow muscle fibers, or medial fast fibers.[28−31] The patterning of somitic cells depends in part on the level and timing of cAMP−protein kinase A (PKA) activity, which inhibits the response to Shh.[25,26,32] Analysis of doubly transgenic embryos expressing both *Tg(ubi:DDcAMP)* and the Shh reporter *Tg(gli:mCherry-NLS)* revealed that N41-GFP signal appeared in Shh-responsive muscle pioneers (mp) and slow muscle cells (smc) (Figure S4A).[33] This colocalization was not evident in the controls with *Tg(ubi:DDcAMP^{R307Q})* or *Tg(ubi:GFP)* (Figure S4B).

There is evidence that the ciliary GPCR Gpr161 negatively regulates Shh signaling by increasing cAMP concentration in the cilium,[34−36] and *gpr161b* is expressed in developing adaxial cells of zebrafish embryos.[37] To determine if the DDcAMP sensor detects cAMP generated by Gpr161 in developing muscle cells, we used CRISPR-Cas9 to generate presumed null mutations in the duplicated genes encoding the Gpr161a and Gpr161b proteins (*gpr161a* and *gpr161b*, Figure S4C). In

accordance with previous work, the number of Shh responsive cells in the somites was increased in the double mutant for *gpr161a$^{st129/129}$* and maternal zygotic MZ*gpr161b$^{128/128}$*, hereafter referred to as "*gpr161* mutants" (Figure 4A, magenta).[36] In *gpr161* mutants, the *Tg(ubi:DDcAMP)* GFP signal in somites was reduced, providing evidence that DDcAMP accurately reports on the reduced levels of endogenous cAMP produced by Gpr161 in developing muscle (Figure 4B,C). Imaging indicated that DDcAMP is detectable in the nucleus and cytoplasm, whereas Gpr161 is most active in cilia.[27,35,38] In an effort to quantify cAMP levels in cilia, a cilium-localizing peptide was appended to the N-terminus of DDcAMP (Arl13b-DDcAMP). The cilia-localized Arl13b-DDcAMP displayed similar levels of GFP signal to the corresponding ciliary control (Arl13b-DDcAMP^{R307Q}), FSK treatment did not significantly affect the GFP signal of either protein (Figure S4D,E), and ciliary DDcAMP signal was similar in wild-type and *gpr161* mutants (Figure 4D,E). These results indicate that the sensor does not specifically detect Gpr161-dependent cAMP in the cilium, perhaps because ciliary localization impedes efficient degradation of the unliganded DDcAMP protein.

Ligand-dependent protein stabilization is a general strategy that has been used to develop a portfolio of reagents that allow users to tunably regulate expression levels of a wide variety of proteins using cell permeable small molecules.[18,39,40] Feng et al. demonstrated that the same strategy could be extended to develop protein-based sensors for secondary metabolites such as progesterone in yeast and digoxin in plants.[17] Given that existing cAMP sensors are not suitable for imaging in living zebrafish, we used ligand-dependent protein stabilization to generate a genetically encoded single wavelength sensor that allows long-term imaging of endogenous cAMP in zebrafish embryos. We identified DDcAMP as a protein sensor that is
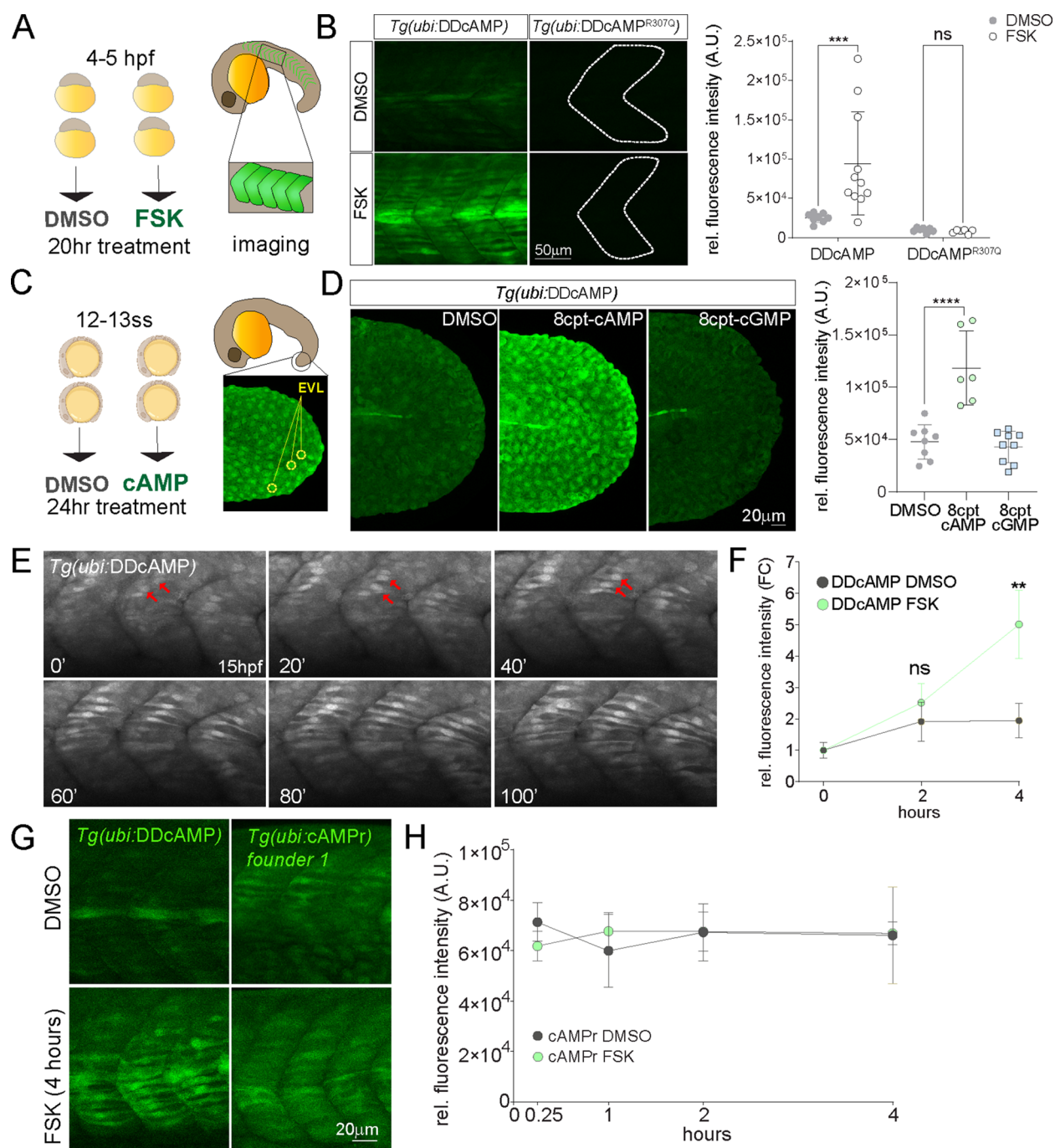
Figure 3. (A) Diagram of DMSO and 20 μM FSK treatment on $Tg(ubi{:}DDcAMP)$ and $Tg(ubi{:}DDcAMP^{R307Q})$ embryos beginning at 4−5 hpf for 20 h. Anterior somites from treated embryos were imaged at 24 hpf, and GFP intensity was measured in somites 7−11. (B) Images of somites from DMSO and FSK-treated $Tg(ubi{:}DDcAMP)$ and $Tg(ubi{:}DDcAMP^{R307Q})$ embryos at 24 hpf. The graph represents the mean fluorescence intensity of five somites per embryo, and each point corresponds to one embryo. Error bars indicate SD: ***$p < 0.001$ by two-way ANOVA (Šidák's multiple comparisons), $n = 6{-}11$ animals for each condition. ns = not significant. AU = arbitrary unit. (C) Diagram of DMSO and 8-cpt-cAMP treatment of $Tg(ubi{:}DDcAMP)$ starting at 12−13 somite stage (12−13ss) and imaged after 24 h of incubation. The tip of the tail was imaged for GFP intensity and the EVLs were quantified. (D) $Tg(ubi{:}DDcAMP)$ embryos from the same clutch were treated with DMSO, 100 μM 8-cpt-cAMP, or 100 μM 8-cpt-cGMP; signal from 20 EVL cells was averaged per animal. Each dot in the graph represents one animal. Error bars indicate SD; ****$p < 0.0001$ one-way ANOVA (with Bonferroni's multiple comparisons), $n = 6{-}9$ animal per condition. AU = arbitrary unit. (E) Frames from a confocal time lapse image with Airyscan 2 processing of $Tg(ubi{:}DDcAMP)$ embryo starting at 15 hpf ($t = 0$ min). One frame every 20 min is shown as representation of the time lapse. GFP-expressing muscle cells are indicated with red arrows. (F) Graph represents the fold change of mean fluorescence intensity measured in five somites per embryo at time 0 and after 2 and 4 h of treatment. Error bars indicate SEM; **$p < 0.01$ two-way ANOVA (with Šidák's multiple comparisons), $n = 6{-}10$ animals for each condition. ns = not significant, FC = fold change. (G) Confocal images of somites from $Tg(ubi{:}DDcAMP)$ and $Tg(ubi{:}cAMPr)$ embryos after 4 h of FSK and DMSO treatment show GFP expression in muscle cells but different response to FSK treatment. (H) Graph represents the mean fluorescence intensity measured in five somites per embryo at the time points indicated. Error bars indicate SEM; there is no significance among the groups; $n = 4{-}5$ animals for each condition.
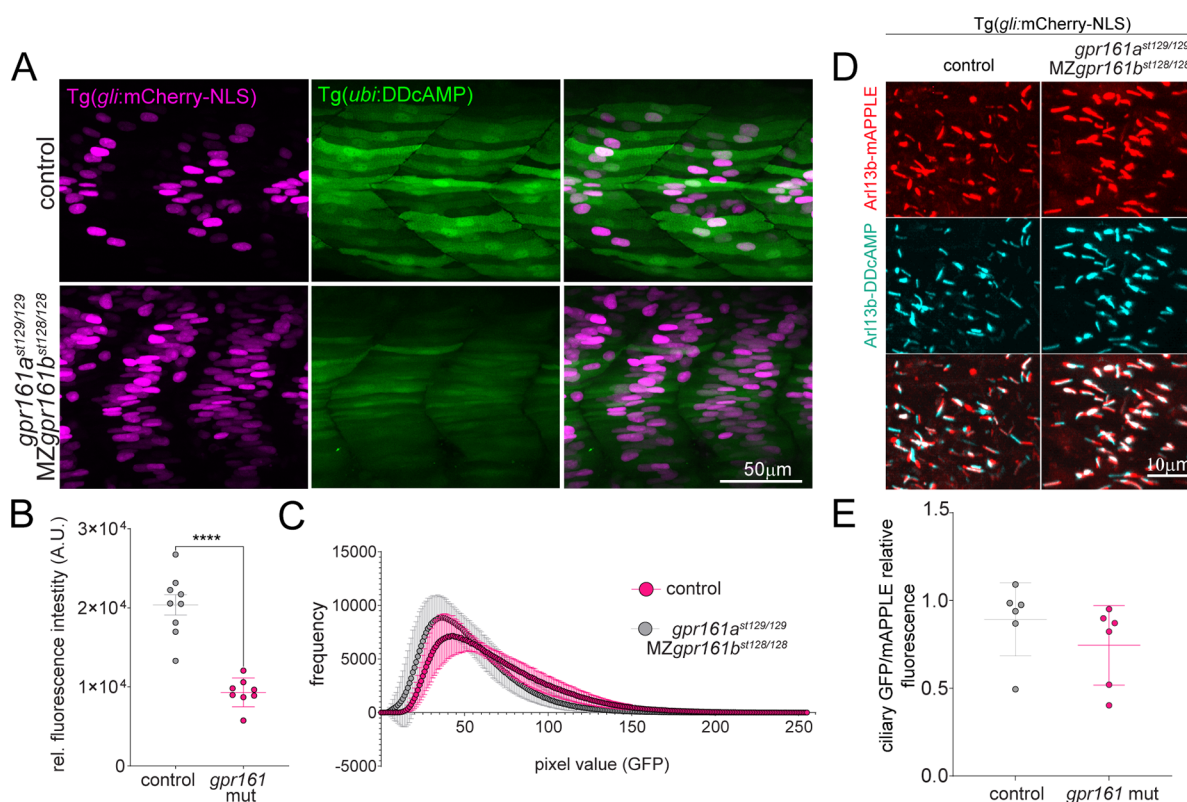
Figure 4. (A) Confocal images of cAMP (green) and Shh reporter (magenta) signals in control fish and double mutants for *gpr161a* (st129 allele) and MZ*gpr161b* (st128 allele). MZ = maternal zygotic. Control fish include *gpr161a*[st129/+], *gpr161b*[128/+] and *gpr161a*[st129/129], *gpr161b*[128/+]. (B) Graphs show GFP fluorescence intensity measured in the somite area corresponding to the muscle pioneers in *Tg*(*gli*:mCherry-NLS); *Tg*(*ubi*:DDcAMP) (control) and in *Tg*(*gli*:mCherry-NLS); *Tg*(*ubi*:DDcAMP); *gpr161a*[st129/129]; MZ*gpr161b*[128/128] (*gpr161* mut) embryos. Error bars indicate SD: ****$p < 0,0001$ by *t*-test. (C) Mean of the pixel values in each image acquired in panel A plotted as a function of their frequency. *gpr161* double mutant fish display darker values compared to the controls. $n = 4-5$ animals per genotype. (D) Magnification of somites from 24 hpf *Tg*(*gli*:mCherry-NLS) control and *Tg*(*gli*:mCherry-NLS); *gpr161a*[st129/129]; MZ*gpr161b*[128/128] embryos injected at one-cell stage with Arl13b-DDcAMP (cyan) and Arl13b-mApple (red cilia). (E) Ratio of ciliary GFP/ciliary mAPPLE in over 20 cilia per animal in *Tg*(*gli*:mCherry-NLS) (control) and *Tg*(*gli*:mCherry-NLS); *gpr161a*[st129/129]; MZ*gpr161b*[128/128] (*gpr161* mut) embryos.

specifically stabilized by cAMP, and we created transgenic fish that ubiquitously express DDcAMP.

DDcAMP specifically responds to the production of cAMP in developing muscle cells. Our analyses suggest that DDcAMP turnover is regulated by cAMP concentration and that this sensor produces a strong GFP signal specifically in response to cAMP. These features enable in vivo time lapse imaging without phototoxicity and bleaching; however DDcAMP is relatively slow to respond to changes in cAMP levels. There is a 3-fold increase in DDcAMP GFP intensity after 4 h of exposure to 20 μM FSK. This time lag presumably reflects the time required for newly translated DDcAMP to be stabilized by cAMP. Thus, DDcAMP is suitable for imaging endogenous cAMP levels in living zebrafish embryos, but it may not be ideal for monitoring changes in cAMP levels that occur over rapid time scales or in subcellular compartments with restricted access to the ubiquitin-proteasome system. DDcAMP has complementary features to other recently developed cAMP sensors, and it will enable new approaches to analyze cAMP in different experimental settings, cell types, and model organisms.

ASSOCIATED CONTENT

Ⓢ Supporting Information

The Supporting Information is available free of charge at https://pubs.acs.org/doi/10.1021/acschembio.2c00333.

Cloning and genotyping primers and sgRNA sequences (XLSX)

Model organisms and strains, recombinant DNA resources, and software and algorithms (XLSX)

Confocal time lapse image of *Tg*(*ubi*:DDcAMP) embryo starting at 15 hpf ($t = 0'$). The embryo is oriented dorsally, with the anterior developing head on top. Developing adaxial cells gradually increase GFP intensity in the somites. The images were taken every 8 minutes for over 7 hours of time lapse (MP4)

Experimental information on CNBD structure, transgene, and pharmacological and genetic validation, details on the experimental procedures for the CNBD selection, transgene generation, and image acquisition (PDF)

■ AUTHOR INFORMATION

Corresponding Author

William S. Talbot − *Department of Developmental Biology, School of Medicine, Stanford University, Stanford, California 94305, United States;* ⓞ orcid.org/0000-0002-2048-7472; Email: wtalbot@stanford.edu

Authors

Mariapaola Sidoli − *Department of Developmental Biology, School of Medicine, Stanford University, Stanford, California 94305, United States*

Ling-chun Chen − *Department of Chemical and Systems Biology, School of Medicine, Stanford University, Stanford, California 94305, United States*

Alexander J. Lu − *Department of Chemical and Systems Biology, School of Medicine, Stanford University, Stanford, California 94305, United States;* ⊙ orcid.org/0000-0003-2868-753X

Thomas J. Wandless − *Department of Chemical and Systems Biology, School of Medicine, Stanford University, Stanford, California 94305, United States*

Complete contact information is available at:
https://pubs.acs.org/10.1021/acschembio.2c00333

Notes
The authors declare no competing financial interest.

■ REFERENCES

(1) Willoughby, D.; Cooper, D. M. F. Organization and Ca2+ Regulation of Adenylyl Cyclases in CAMP Microdomains. *Physiol Rev.* **2007**, *87* (3), 965−1010.

(2) Morozov, A.; Muzzio, I. A.; Bourtchouladze, R.; Van-Strien, N.; Lapidus, K.; Yin, D.; Winder, D. G.; Adams, J. P.; Sweatt, J. D.; Kandel, E. R. Rap1 Couples CAMP Signaling to a Distinct Pool of P42/44MAPK Regulating Excitability, Synaptic Plasticity, Learning, and Memory. *Neuron* **2003**, *39* (2), 309−325.

(3) Lee, D. Global and Local Missions of CAMP Signaling in Neural Plasticity, Learning, and Memory. *Front Pharmacol* **2015**, *6*, 161.

(4) Surdo, N. C.; Berrera, M.; Koschinski, A.; Brescia, M.; Machado, M. R.; Carr, C.; Wright, P.; Gorelik, J.; Morotti, S.; Grandi, E. M.; et al. FRET Biosensor Uncovers CAMP Nano-Domains at β-Adrenergic Targets That Dictate Precise Tuning of Cardiac Contractility. *Nat. Commun.* **2017**, *8* (1), 15031.

(5) Koschinski, A.; Zaccolo, M. Activation of PKA in Cell Requires Higher Concentration of CAMP than in Vitro : Implications for Compartmentalization of CAMP Signalling. *Sci. Rep* **2017**, *7* (1), 1−12.

(6) Johnson, J.-L. F.; Leroux, M. R. cAMP and cGMP Signaling: Sensory Systems with Prokaryotic Roots Adopted by Eukaryotic Cilia. *Trends Cell Biol.* **2010**, *20* (8), 435−444.

(7) Zaccolo, M.; Zerio, A.; Lobo, M. J. Subcellular Organization of the CAMP Signaling Pathway. *Pharmacol Rev.* **2021**, *73* (1), 278−309.

(8) Sprenger, J. U.; Nikolaev, V. O. Biophysical Techniques for Detection of CAMP and CGMP in Living Cells. *Int. J. Mol. Sci.* **2013**, *14* (4), 8025−8046.

(9) Zhao, M.; Wan, X.; Li, Y.; Zhou, W.; Peng, L. Multiplexed 3D FRET Imaging in Deep Tissue of Live Embryos. *Sci. Rep* **2015**, *5* (1), 13991.

(10) Kim, N.; Shin, S.; Bae, S. W. CAMP Biosensors Based on Genetically Encoded Fluorescent/Luminescent Proteins. *Biosensors (Basel)* **2021**, *11* (2), 39.

(11) Odaka, H.; Arai, S.; Inoue, T.; Kitaguchi, T. Genetically-Encoded Yellow Fluorescent CAMP Indicator with an Expanded Dynamic Range for Dual-Color Imaging. *PLoS One* **2014**, *9* (6), e100252.

(12) Hackley, C. R.; Mazzoni, E. O.; Blau, J. cAMPr: A Single-Wavelength Fluorescent Sensor for Cyclic AMP. *Sci. Signal.* **2018**, *11* (520), eaah3738.

(13) Ohta, Y.; Furuta, T.; Nagai, T.; Horikawa, K. Red Fluorescent CAMP Indicator with Increased Affinity and Expanded Dynamic Range. *Sci. Rep* **2018**, *8* (1), 1866.

(14) Harada, K.; Ito, M.; Wang, X.; Tanaka, M.; Wongso, D.; Konno, A.; Hirai, H.; Hirase, H.; Tsuboi, T.; Kitaguchi, T. Red Fluorescent Protein-Based CAMP Indicator Applicable to Optogenetics and in Vivo Imaging. *Sci. Rep* **2017**, *7* (1), 7351.

(15) Oe, Y.; Wang, X.; Patriarchi, T.; Konno, A.; Ozawa, K.; Yahagi, K.; Hirai, H.; Tsuboi, T.; Kitaguchi, T.; Tian, L.; et al. Distinct Temporal Integration of Noradrenaline Signaling by Astrocytic Second Messengers during Vigilance. *Nat. Commun.* **2020**, *11* (1), 471.

(16) Li, F.; Sami, A.; Noristani, H. N.; Slattery, K.; Qiu, J.; Groves, T.; Wang, S.; Veerasammy, K.; Chen, Y. X.; Morales, J.; et al. Glial Metabolic Rewiring Promotes Axon Regeneration and Functional Recovery in the Central Nervous System. *Cell Metab* **2020**, *32* (5), 767−785.e7.

(17) Feng, J.; Jester, B. W.; Tinberg, C. E.; Mandell, D. J.; Antunes, M. S.; Chari, R.; Morey, K. J.; Rios, X.; Medford, J. I.; Church, G. M.; et al. A General Strategy to Construct Small Molecule Biosensors in Eukaryotes. *eLife Sciences* **2015**, *4*, e10606.

(18) Banaszynski, L. A.; Chen, L.-C.; Maynard-Smith, L. A.; Ooi, A. G. L.; Wandless, T. J. A Rapid, Reversible, and Tunable Method to Regulate Protein Function in Living Cells Using Synthetic Small Molecules. *Cell* **2006**, *126* (5), 995−1004.

(19) Iwamoto, M.; Björklund, T.; Lundberg, C.; Kirik, D.; Wandless, T. J. A General Chemical Method to Regulate Protein Stability in the Mammalian Central Nervous System. *Chem. Biol.* **2010**, *17* (9), 981−988.

(20) Navarro, R.; Chen, L.-C.; Rakhit, R.; Wandless, T. J. A Novel Destabilizing Domain Based on a Small-Molecule Dependent Fluorophore. *ACS Chem. Biol.* **2016**, *11* (8), 2101−2104.

(21) Clayton, G. M.; Silverman, W. R.; Heginbotham, L.; Morais-Cabral, J. H. Structural Basis of Ligand Activation in a Cyclic Nucleotide Regulated Potassium Channel. *Cell* **2004**, *119* (5), 615−627.

(22) Mukherjee, S.; Jansen, V.; Jikeli, J. F.; Hamzeh, H.; Alvarez, L.; Dombrowski, M.; Balbach, M.; Strünker, T.; Seifert, R.; Kaupp, U. B.; et al. A Novel Biosensor to Study CAMP Dynamics in Cilia and Flagella. *eLife Sciences* **2016**, *5*, e14052.

(23) Schünke, S.; Stoldt, M.; Lecher, J.; Kaupp, U. B.; Willbold, D. Structural Insights into Conformational Changes of a Cyclic Nucleotide-Binding Domain in Solution from Mesorhizobium Loti K1 Channel. *Proc. Natl. Acad. Sci. U.S.A.* **2011**, *108* (15), 6121−6126.

(24) Mosimann, C.; Kaufman, C. K.; Li, P.; Pugach, E. K.; Tamplin, O. J.; Zon, L. I. Ubiquitous Transgene Expression and Cre-Based Recombination Driven by the Ubiquitin Promoter in Zebrafish. *Development* **2011**, *138* (1), 169−177.

(25) Du, S. J.; Devoto, S. H.; Westerfield, M.; Moon, R. T. Positive and Negative Regulation of Muscle Cell Identity by Members of the Hedgehog and TGF-Beta Gene Families. *J. Cell Biol.* **1997**, *139* (1), 145−156.

(26) Barresi, M. J.; Stickney, H. L.; Devoto, S. H. The Zebrafish Slow-Muscle-Omitted Gene Product Is Required for Hedgehog Signal Transduction and the Development of Slow Muscle Identity. *Development* **2000**, *127* (10), 2189−2199.

(27) Truong, M. E.; Bilekova, S.; Choksi, S. P.; Li, W.; Bugaj, L. J.; Xu, K.; Reiter, J. F. Vertebrate Cells Differentially Interpret Ciliary and Extraciliary CAMP. *Cell* **2021**, *184* (11), 2911−2926.e18.

(28) Regard, J. B.; Malhotra, D.; Gvozdenovic-Jeremic, J.; Josey, M.; Chen, M.; Weinstein, L. S.; Lu, J.; Shore, E. M.; Kaplan, F. S.; Yang, Y. Activation of Hedgehog Signaling by Loss of GNAS Causes Heterotopic Ossification. *Nat. Med.* **2013**, *19* (11), 1505−1512.

(29) Lee, R. T. H.; Zhao, Z.; Ingham, P. W. Hedgehog Signalling. *Development* **2016**, *143* (3), 367−372.

(30) Hirsinger, E.; Stellabotte, F.; Devoto, S. H.; Westerfield, M. Hedgehog Signaling Is Required for Commitment but Not Initial Induction of Slow Muscle Precursors. *Dev. Biol.* **2004**, *275* (1), 143−157.

(31) Ingham, P. W.; Kim, H. R. Hedgehog Signalling and the Specification of Muscle Cell Identity in the Zebrafish Embryo. *Exp. Cell Res.* **2005**, *306* (2), 336−342.

(32) Huang, P.; Schier, A. F. Dampened Hedgehog Signaling but Normal Wnt Signaling in Zebrafish without Cilia. *Development* **2009**, *136* (18), 3089−3098.

(33) Mich, J. K.; Payumo, A. Y.; Rack, P. G.; Chen, J. K. In Vivo Imaging of Hedgehog Pathway Activation with a Nuclear Fluorescent Reporter. *PLoS One* **2014**, *9* (7), e103661.

(34) Mukhopadhyay, S.; Wen, X.; Ratti, N.; Loktev, A.; Rangell, L.; Scales, S. J.; Jackson, P. K. The Ciliary G-Protein-Coupled Receptor Gpr161 Negatively Regulates the Sonic Hedgehog Pathway via CAMP Signaling. *Cell* **2013**, *152* (1−2), 210−223.

(35) Bachmann, V. A.; Mayrhofer, J. E.; Ilouz, R.; Tschaikner, P.; Raffeiner, P.; Röck, R.; Courcelles, M.; Apelt, F.; Lu, T.-W.; Baillie.; et al. Gpr161 Anchoring of PKA Consolidates GPCR and CAMP Signaling. *Proc. Natl. Acad. Sci. U.S.A.* **2016**, *113* (28), 7786−7791.

(36) Tschaikner, P. M.; Regele, D.; Röck, R.; Salvenmoser, W.; Meyer, D.; Bouvier, M.; Geley, S.; Stefan, E.; Aanstad, P. Feedback Control of the Gpr161-Gαs-PKA Axis Contributes to Basal Hedgehog Repression in Zebrafish. *Development* **2021**, *148* (4), dev192443.

(37) Wang, M.; Li, P.; Wang, H.; Dong, L.; Wu, C.; Zhao, Z. Identification and Spatiotemporal Expression of Gpr161 Genes in Zebrafish. *Gene* **2020**, *730*, 144303.

(38) Hwang, S.-H.; Somatilaka, B. N.; White, K.; Mukhopadhyay, S. Ciliary and Extraciliary Gpr161 Pools Repress Hedgehog Signaling in a Tissue-Specific Manner. *eLife* **2021**, *10*, e67121.

(39) Egeler, E. L.; Urner, L. M.; Rakhit, R.; Liu, C. W.; Wandless, T. J. Ligand-Switchable Substrates for a Ubiquitin-Proteasome System. *J. Biol. Chem.* **2011**, *286* (36), 31328−31336.

(40) Miyazaki, Y.; Imoto, H.; Chen, L.; Wandless, T. J. Destabilizing Domains Derived from the Human Estrogen Receptor. *J. Am. Chem. Soc.* **2012**, *134* (9), 3942−3945.